Int. J. Solids Structures, 1977, Vol. 13, pp. 63–74. Pergamon Press. Printed in Great Britain.

TRANSIENT RESPONSE OF A LAYERED ELASTIC HALF SPACE SUBJECTED TO A RECIPROCATING ANTI-PLANE SHEAR LOAD

KAZUMI WATANABE
Mechanical Engineering II, Tohoku University, Sendai, 980 Japan

(*Received* 16 *April* 1976; *revised* 14 *July* 1976)

Abstract—The well-known Cagniard's technique seems very useful for analyzing the transient problem of an elastic body subjected to a moving load with uniform velocity, but, in the cases of non-uniform velocity it would be difficult to apply the technique directly to analyze the problem. For such cases, instead of the technique, the convolution theorem of the Laplace transform or the dynamic Betti-Rayleigh reciprocal theorem has been applied usefully by many authors.

In this paper, an inversion scheme which enables us to apply the Cagniard's technique directly to those difficult problems is presented by solving the problem of a reciprocating anti-plane shear load applied to a layered elastic half space. In this treatment it will be found clearly that our technique is simpler and more systematic than any other techniques for solving the problem. Numerical results are shown in the form of curves and the wave-front singularities are also investigated.

1. INTRODUCTION

All branches of recent transport have advanced because of increasing speeds and weights of vehicles. As a result, machine and structure with moving vehicles have been subjected to dynamic behaviours more than ever. That is why the problems concerning a moving load attract attentions of researchers in this field. We can find a comprehensive treatment concerning these problems in Fŕyba's book[1].

For example, the problems of a steadily moving load on the surface of an elastic half space are treated in Refs [2–4] and the transient problems of this type are also considered by Payton[5], Ang[6], Gakenheimer[7], etc. However, these analyses are limited to such problems as those of a moving load with uniform velocity. It appears that there have been only a few paper concerning the load with non-uniform velocity. We can cite the work of Beitin[8] as a typical example. He has obtained the surface response of an elastic half space subjected to a decelerating load. Although Miles[9] has considered the response due to a non-uniformly expanding blast wave, he has not given any numerical examples. On the other hand, Stronge[10] and Myers[11] have analyzed the transient behaviour of a liquid half space due to accelerating and decelerating loads, respectively. These solutions are valid for the problem of an anti-plane shear load in the theory of elasticity.

The studies just mentioned above are limited to such problem that the load moves forward and never returns to its initial position. But, there are so many machines and structural constituents subjected to a reciprocating load such as a reciprocating engine. Then, it will be desirable to consider the response due to the load. Notwithstanding the importance of this problem, there have been no studies except Ohyoshi's[12] relating the problem. He has obtained the steady-state solutions for an elastic half space. So, in the previous paper[13] the author has tried to establish an inversion scheme for solving the problem of a moving load with an arbitrary variation of velocity and obtained the transient response of an elastic half space subjected to the reciprocating anti-plane shear load.

Besides, for a layered media the steady-state responses due to the uniformly moving load were investigated by Sackman[14] and Wright and Baron[15]. The transient response due to a stationary load was studied by Knopoff[16] and the author[17]. However, there also have been little papers for the traisient response due to a non-uniformly moving load.

While the problem of the uniformly moving load has been solved concisely by the application of the well-known Cagniard's technique[6, 7], there has been no direct applications of it to the

problem of non-uniformly moving load. Instead of the technique, the convolution theorem of the Laplace transform[10, 11] and the dynamic Betti-Rayleigh reciprocal theorem have been used availably. Owing to this, the analysis has been always complicated mathematically. To overcome the difficulty, taking into account of the fact that the response at an observing point is given by the sum of disturbance generated by a wave emanating from a loaded point, the author made a change in the course of the Laplace transform and developed an inversion scheme as shown in [13]. The scheme has led the Cagniard's technique to be available and simpler than any other analyses.

In this paper we study the transient response of a layered elastic half space subjected to a reciprocating anti-plane shear load in order to develop the scheme further. The load is suddenly applied and subsequently moves in an interval on the surface of the layer as a trigonometric function of time. The exact response on the interface is obtained in terms of single integration. It is shown that the discontinuities in the displacement take place only for the case when the maximum velocity of the load is greater than that of SH-wave of the layer. In this case the displacement has a finite jump on a leading front and has a logarithmic discontinuity immediately behind the front emanating from a sonic point. Numerical calculations are carried out for a case of maximum velocity and the results are shown graphically.

2. FORMULATION

Let us consider a layered elastic half space shown in Fig. 1 based on a Cartesian coordinates system (x, y, z). An elastic layer with thickness h and an elastic half space having dissimilar material properties are bonded together at a common boundary $y = 0, 0 \leqq |x| < \infty$. The interiors of the layer and the half space are defined by $-h \leqq y < 0$ and $y > 0$, respectively. Material properties, components of stress and displacement are denoted by subscripts 1 for the layer and by 2 for the half space.

An anti-plane shear load of magnitude P is suddenly applied and subsequently moves in an interval $0 \leqq |x| \leqq l$ on the surface of the layer as a trigonometric function of time. It is also assumed that the load is removed from the layer just after time t_0. Then, the load is given by

$$\sigma_{yz1} = P\delta(x - l \sin \omega t)H(t)H(t_0 - t); \quad \text{at} \quad y = -h \tag{1}$$

where ω is the angular frequency of the reciprocating motion, and $\delta(\ )$ and $H(\ )$ are Dirac's delta and Heaviside's unit step functions, respectively. The velocity of the load is given by

$$v = l\omega \cos \omega t \tag{2}$$

Since the load is only an anti-plane shear load, the resulting response of the layered half space is governed by the equations,

$$W_{j,xx} + W_{j,yy} = c_j^{-2} W_{j,tt} \tag{3}$$
$$c_j = (\mu_j/\rho_j)^{1/2}; \quad j = 1, 2$$

where W_j is the displacement in the direction of z-axis and where μ_j and ρ_j are shear modulus and density, respectively. The repeated subscripts do not mean the convention of summation

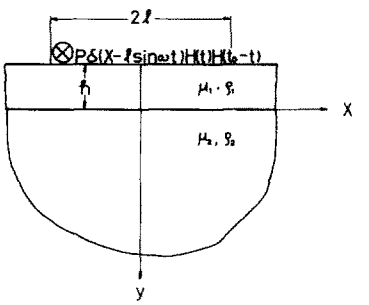

Fig. 1. The layered half space subjected to a reciprocating anti-plane shear load.

throughout the paper. Non-vanishing components of stress are defined by

$$\sigma_{xzj} = \mu_j W_{j'x}, \quad \sigma_{yzj} = \mu_j W_{j'y} \tag{4}$$

Then, assuming the quiescent conditions

$$W_j|_{t=0} = W_{j't}|_{t=0} = 0 \tag{5}$$

we apply the Laplace and Fourier transforms defined by

$$f^*(s) = \int_0^\infty f(t) \exp(-st)\, dt; \quad \text{Laplace transform} \tag{6}$$

$$\bar{f}(\xi) = \int_{-\infty}^\infty f(x) \exp(i\xi x)\, dx; \quad \text{Fourier transform} \tag{7}$$

to eqns (1), (3) and (4) and to the continuity conditions on the interface,

$$\sigma_{yz1} = \sigma_{yz2}, \quad W_1 = W_2; \quad \text{at } y = 0 \tag{8}$$

Following the inversion scheme shown in [13], we leave the transform of eqn (1) in the form of the Laplace transform as

$$\bar{\sigma}^*_{yz1}|_{y=-h} = P \int_0^{t_0} \exp(i\xi l \sin \omega t' - st')\, dt' \tag{9}$$

The evaluation of the above integral is very simple and yields

$$\bar{\sigma}^*_{yz1}|_{y=-h} = P \sum_{n=-\infty}^{\infty} \frac{J_n(\xi l)}{in\omega - s} [\exp\{t_0(in\omega - s) - 1\} - 1] \tag{10}$$

This expression is not desirable because of the difficulty of applying the Cagniard's technique. Notwithstanding the use of the integral representation of the Bessel function $J_n(\xi l)$, both the Cagniard's technique and the convolution theorem of the Laplace transform are applied and the solution obtained will be somewhat complicated form of infinite series involving integration.

Therefore, we employ the form of eqn (9) so that we can apply the Cagniard's technique directly and can obtain a concise solution. Succeeding Fourier inversion of the interface displacement is given by [17] as

$$W^*(x, s) = -\frac{P}{\pi} \sum_{n=0}^{\infty} \int_0^{t_0} dt' \int_{-\infty}^{\infty} \frac{1}{\mu_1\beta_1 + \mu_2\beta_2} \left(\frac{\mu_1\beta_1 - \mu_2\beta_2}{\mu_1\beta_1 + \mu_2\beta_2}\right)^n \times \exp\{-i\xi(x - l \sin \omega t') - st' - (2n+1)\beta_1 h\}\, d\xi \tag{11}$$

$$\beta_j = (\xi^2 + s^2/c_j^2)^{1/2}, \quad Re(\beta_j) \geqq 0$$

where $W(x, t)$ is defined by

$$W(x, t) = W_1|_{y=0^-} = W_2|_{y=0^+} \tag{12}$$

As shown in [16, 17], the application of the Cagniard's technique leads eqn (11) to an alternate form of integration along the Cagniard's contour shown in Fig. 2. That is

$$-\frac{\pi\mu_1}{P} W^*(x, s) = \sum_{n=0}^{\infty} W_n^*(x, s) \tag{13}$$

$$W_n^*(x, s) = \int_0^{\eta_0} d\eta \int_{h\tau_n(\eta)/c_1}^{\infty} \exp(-st) \left\{ T_n(\zeta_n^+) \frac{d\zeta_n^+}{d\tau} - T_n(\zeta_n^-) \frac{d\zeta_n^-}{d\tau} \right\} dt \tag{14}$$

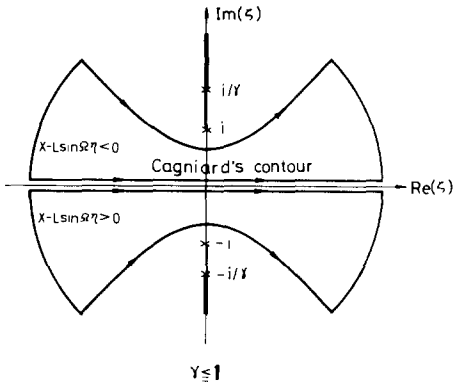

Fig. 2. Cagniard's contours ($\gamma \leqq 1$).

where

$$\tau_n(\eta) = \eta + \sqrt{(X - L\sin\Omega\eta)^2 + (2n+1)^2} \tag{15}$$

$$\zeta_n^{\pm} = \frac{-i(\tau-\eta)(X - L\sin\Omega\eta) \pm (2n+1)\sqrt{(\tau-\eta)^2 - (X - L\sin\Omega\eta)^2 - (2n+1)^2}}{(X - L\sin\Omega\eta)^2 + (2n+1)^2} \tag{16}$$

$$T_n(\zeta) = \frac{1}{\alpha_1 + \lambda\alpha_2}\left(\frac{\alpha_1 - \lambda\alpha_2}{\alpha_1 + \lambda\alpha_2}\right)^n \tag{17}$$

$$\alpha_1 = (\zeta^2+1)^{1/2}, \quad \alpha_2 = (\zeta^2 + 1/\gamma^2)^{1/2}$$

and the following dimensionless quantities are introduced,

$$\left.\begin{aligned} X = x/h, \quad \tau = c_1 t/h, \quad \eta_0 = c_1 t_0/h, \quad L = l/h \\ \lambda = \mu_2/\mu_1, \quad \gamma = c_2/c_1, \quad \Omega = h\omega/c_1 \end{aligned}\right\} \tag{18}$$

with $0 < \gamma \leqq 1$ assumed for convenience.

3. LAPLACE INVERSION

It is clear that the first integral in eqn (14) is just the same form as the Laplace transform. Thus, the subsequent step is to change the order of the double integration so that we can obtain the inversion by inspection. So, let us consider the inversion of the general n-th term $W_n^*(x, s)$ in eqn (13).

In the first, the function $\tau = \tau_n(\eta)$ given by eqn (15), which is the lower bound of the first integral, and its inverse function defined by $\eta = \tau_n^{-1}(\tau)$ should be examined. If the derivative of $\tau_n(\eta)$ with respect to η,

$$\frac{d\tau_n(\eta)}{d\eta} = 1 - \frac{L\Omega(X - L\sin\Omega\eta)\cos\Omega\eta}{\sqrt{(X - L\sin\Omega\eta)^2 + (2n+1)^2}} \tag{19}$$

is positive for all $\eta (0 \leqq \eta \leqq \eta_0)$, the inverse function is a single-valued function and for a given τ we can determine η uniquely. In this case the order is changed easily and eqn (14) is reduced to the form of the Laplace transform. (The region of support for the double integration is shown by the region above the thick curve $\tau = \tau_n(\eta)$ in Fig. 4a). That is

$$W_n^*(x, s) = \left\{\int_{h\tau_n(0)/c_1}^{h\tau_n(\eta_0)/c_1} dt \int_0^{\tau_n^{-1}(\tau)} + \int_{h\tau_n(\eta_0)/c_1}^{\infty} dt \int_0^{\eta_0}\right\}$$

$$\times \exp(-st)\left\{T_n(\zeta_n^+)\frac{d\zeta_n^+}{d\tau} - T_n(\zeta_n^-)\frac{d\zeta_n^-}{d\tau}\right\} D\eta \tag{20}$$

By inspection, we obtain the inversion in terms of single integration as

$$W(x,t)=\left[H\{\tau_n(\eta_0)-\tau\}H\{\tau-\sqrt{X^2+(2n+1)^2}\}\int_0^{\tau_n^{-1}(\tau)}+H\{\tau-\tau_n(\eta_0)\}\int_0^{\eta_0}\right]$$
$$\times\left\{T_n(\zeta_n^+)\frac{d\zeta_n^+}{d\tau}-T_n(\zeta_n^-)\frac{d\zeta_n^-}{d\tau}\right\}d\eta \tag{21}$$

It is evident that the integrand in eqn (21) shows the disturbance caused by a wave originated from a loaded point at time η and that the integration implies the sum of the disturbance.

Response on the center axis of the reciprocating motion

If the function $\tau_n(\eta)$ has extremum, the inverse function $\eta=\tau_n^{-1}(\tau)$ is a multi-valued function and the inversion of eqn (14) becomes more complicated. Then, for the sake of the simplicity we confine our attention to the response at the point $X=0$. The point is on the center axis of the reciprocating motion. Thus, putting $X=0$ in eqns (15) and (19), we get

$$\tau=\tau_n(\eta)=\eta+\sqrt{L^2\sin^2\Omega\eta+(2n+1)^2} \tag{22}$$

$$\frac{d\tau_n(\eta)}{d\eta}=1+\frac{L^2\Omega\sin(2\Omega\eta)}{2\sqrt{L^2\sin^2\Omega\eta+(2n+1)^2}} \tag{23}$$

Considering these equations well, we easily have the following conclusions: (i) if $1/\Omega\geqq\sqrt{(2n+1)^2+L^2}-(2n+1)$, $\tau_n(\eta)$ is a monotonically increasing function and $\eta=\tau_n^{-1}(\tau)$ is a single-valued function, (ii) if $1/\Omega<\sqrt{(2n+1)^2+L^2}-(2n+1)$, $\tau_n(\eta)$ has extremum and $\eta=\tau_n^{-1}(\tau)$ is a multi-valued function.

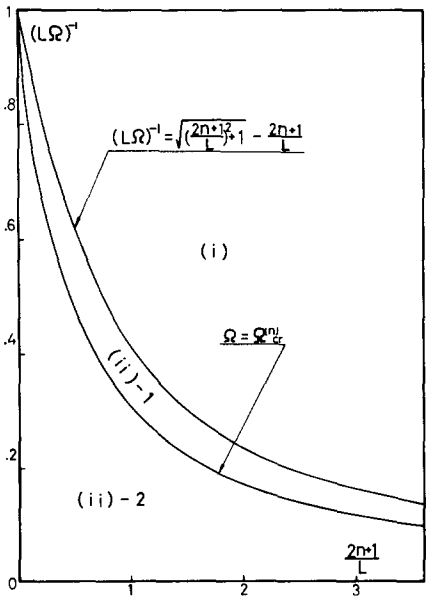

Fig. 3. The graphical classification of the cases (i), (ii)–1 and (ii)–2.

In the case (i) it is evident that the Laplace inversion of eqn (14) is given by eqn (21) with substitution of $X=0$, however, in (ii) the expression of eqn (21) is not acceptable because of the multi-valuedness of the inverse function. Then, the following analysis is set on the latter case.

As eqns (2) and (23) show us that the velocity of the load and $d\tau_n(\eta)/d\eta$ vary with period $2\pi/\Omega$ and π/Ω, respectively, it is sufficient to proceed the analysis for the first one period, $\eta_0=2\pi/\Omega$. (The solution of the longer applied time will be obtained by superposing the solution obtained here with shifting of time.) With this assumption, $\eta_0=2\pi/\Omega$, the case (ii) is decomposed

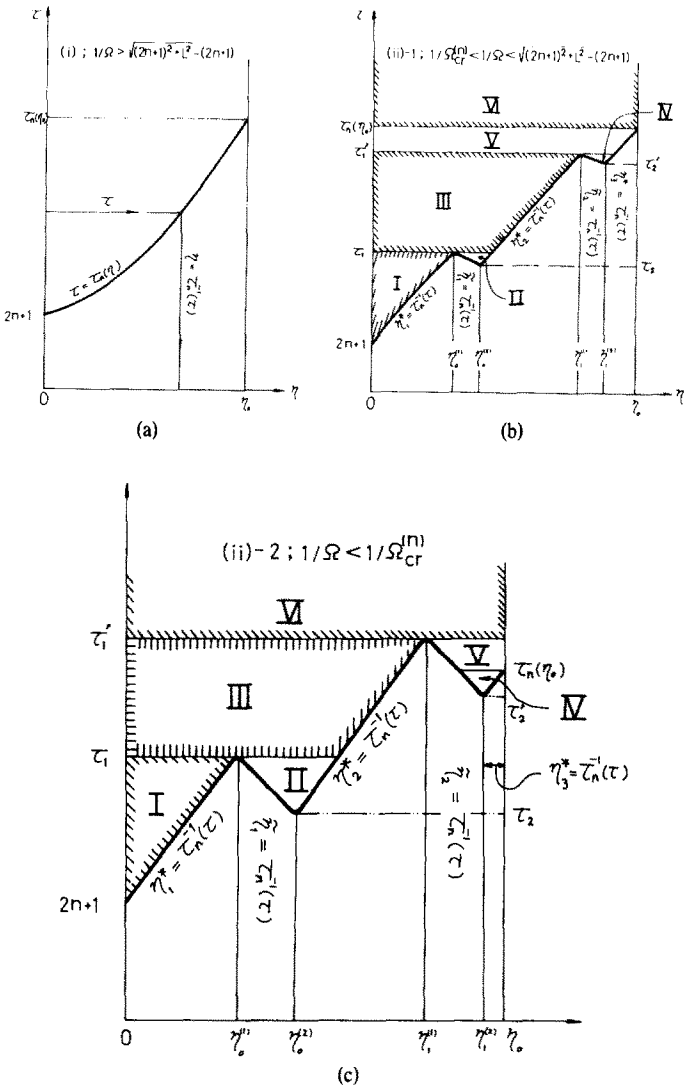

Fig. 4. The region of support for the double integration in eqn (14) ($\eta_0 = 2\pi/\Omega$).

into still two more cases. They are

(ii)–1; $1/\Omega_{cr}^{(n)} \leqq 1/\Omega < \sqrt{(2n+1)^2+L^2}-(2n+1)$; $\tau_n(\eta_1^{(1)}) \leqq \tau_n(\eta_0)$

(ii)–2; $1/\Omega_{cr}^{(n)} > 1/\Omega > 0$; $\tau_n(\eta_1^{(1)}) > \tau_n(\eta_0)$

where $\eta_j^{(1)}$ and $\eta_j^{(2)}$ are the maxima and the minima points of $\tau_n(\eta)$, respectively;

$$\eta_j^{(1)} = \frac{1}{\Omega}\left[\pi j + \sin^{-1}\sqrt{\frac{1}{2}\left\{1 - \frac{1}{L^2\Omega^2} + \sqrt{\left[\left(1-\frac{1}{L^2\Omega^2}\right)^2 - \frac{4}{L^2\Omega^2}\left(\frac{2n+1}{L}\right)^2\right]}\right\}}\right] \tag{24}$$

$$\eta_j^{(2)} = \frac{1}{\Omega}\left[\pi j + \sin^{-1}\sqrt{\frac{1}{2}\left\{1 - \frac{1}{L^2\Omega^2} - \sqrt{\left[\left(1-\frac{1}{L^2\Omega^2}\right)^2 - \frac{4}{L^2\Omega^2}\left(\frac{2n+1}{L}\right)^2\right]}\right\}}\right] \tag{25}$$

$$\frac{\pi}{2} < \sin^{-1}(\ ) < \pi, \quad j = 0, 1, 2, \ldots$$

and $\Omega_{cr}^{(n)}$ satisfies the condition of $\tau_n(\eta_1^{(1)}) = \tau_n(\eta_0 = 2\pi/\Omega)$. The classification of these is shown in Fig. 3 graphically.

Now, let us consider the inversion for the case (ii)–1. The region of support for the double

integration is shown in Fig. 4b. In order to change the order, we devide it into six parts, I, II, III, ..., VI, as shown in the figure and introduce the following notations, for convenience,

$$\left.\begin{matrix}\eta_1^* \\ \eta_2^* \\ \eta_3^*\end{matrix}\right\} = \tau_n^{-1}(\tau)\left.\begin{matrix}; & 0<\eta_1^*<\eta_0^{(1)} \\ ; & \eta_0^{(2)}<\eta_2^*<\eta_1^{(1)} \\ ; & \eta_1^{(2)}<\eta_3^*<\eta_0\end{matrix}\right. \tag{26}$$

$$\left.\begin{matrix}\tilde{\eta}_1 \\ \tilde{\eta}_2\end{matrix}\right\} = \tau_n^{-1}(\tau)\left.\begin{matrix}; & \eta_0^{(1)}<\tilde{\eta}_1<\eta_0^{(2)} \\ ; & \eta_1^{(1)}<\tilde{\eta}_2<\eta_1^{(2)}\end{matrix}\right. \tag{27}$$

$$\tau_1 = \tau_n(\eta_0^{(1)}), \quad \tau_1' = \tau_n(\eta_1^{(1)}), \quad \tau_2 = \tau_n(\eta_0^{(2)}), \quad \tau_2' = \tau_n(\eta_1^{(2)}) \tag{28}$$

Then, it is a simple matter to change the order for each part. Equation (14) is rewritten as

$$\begin{aligned} W_n^*(0,s) = \Bigg[& \int_{h\tau_n(0)/c_1}^{h\tau_1/c_1} \mathrm{d}\tau \int_0^{\eta_1^*} + \int_{h\tau_2/c_1}^{h\tau_1/c_1} \mathrm{d}t \int_{\tilde{\eta}}^{\eta_2^*} + \int_{h\tau_1'/c_1}^{h\tau_1/c_1} \mathrm{d}t \int_0^{\eta_2^*} \\ & + \int_{h\tau_2/c_1}^{h\tau_1'/c_1} \mathrm{d}t \int_{\tilde{\eta}_2}^{\eta_3^*} + \int_{h\tau_1/c_1}^{h\tau_n(\eta_0)/c_1} \mathrm{d}t \int_0^{\eta_3^*} + \int_{h\tau_n(\eta_0)/c_1}^{\infty} \mathrm{d}t \int_0^{\eta_0} \Bigg] \\ & \times \exp(-st)\left\{ T_n(\zeta_n^+)\frac{\mathrm{d}\zeta_n^+}{\mathrm{d}\tau} - T_n(\zeta_n^-)\frac{\mathrm{d}\zeta_n^-}{\mathrm{d}\tau}\right\}\mathrm{d}\eta \end{aligned} \tag{29}$$

and the inversion of this is

$$\begin{aligned} W_n(0,t) = \Bigg[& H(\tau_1-\tau)\left\{ H(\tau-2n-1)\int_0^{\eta_1^*} + H(\tau-\tau_2)\int_{\tilde{\eta}_1}^{\eta_2^*}\right\} \\ & + H(\tau_1'-\tau)\left\{ H(\tau-\tau_1)\int_0^{\eta_2^*} + H(\tau-\tau_2')\int_{\tilde{\eta}_2}^{\eta_3^*}\right\} \\ & + H(\tau-\tau_1')H\{\tau_n(\eta_0)-\tau\}\int_0^{\eta_3^*} + H\{\tau-\tau_n(\eta_0)\}\int_0^{\eta_0}\Bigg] \\ & \times\left\{ T_n(\zeta_n^+)\frac{\zeta_n^+}{\mathrm{d}\tau} - T_n(\zeta_n^-)\frac{\zeta_n^-}{\mathrm{d}\tau}\right\}\mathrm{d}\eta \end{aligned} \tag{30}$$

Similar procedures are applied to the case (ii)–2. For the case the region of support is also shown in Fig. 4c and the inversion yields

$$\begin{aligned} W_n(0,t) = \Bigg[& H(\tau_1-\tau)\left\{ H(\tau-2n-1)\int_0^{\eta_1^*} + H(\tau-\tau_2)\int_{\tilde{\eta}_1}^{\eta_2^*}\right\} \\ & + H(\tau_1'-\tau)\left[H(\tau-\tau_1)\int_0^{\eta_2^*} + H\{\tau-\tau_n(\eta_0)\}\int_{\tilde{\eta}_2}^{\eta_0}\right] \\ & + H(\tau-\tau_2')H\{\tau_n(\eta_0)-\tau\}\int_{\tilde{\eta}_2}^{\eta_3^*} + H(\tau-\tau_1')\int_0^{\eta_0}\Bigg] \\ & \times\left\{ T_n(\zeta_n^+)\frac{\mathrm{d}\zeta_n^+}{\mathrm{d}\tau} - T_n(\zeta_n^-)\frac{\mathrm{d}\zeta_n^-}{\mathrm{d}\tau}\right\}\mathrm{d}\eta \end{aligned} \tag{31}$$

Consequently, the inversion of eqn (14) has just been obtained in terms of single integration for all combinations of L, and n and the response at the point $X = 0$ on the interface is given by

$$-\frac{\pi\mu}{P}W(0,t) = \sum_{n=0}^{\infty} W_n(0,t) \tag{32}$$

where $W_n(0,t)$ must be chosen appropriately from eqns (21), (30) and (31).

4. WAVE ANALYSIS

In this section we shall consider the physical meanings of the cases (i) and (ii) and discuss the discontinuities in the displacement at an observing point where the wavefronts cross the center axis of the reciprocating motion. Although the amplitude is desirable for all of the wavefront, it is expected that the type of the discontinuity or order of singularity for those wavefront curvatures is identical because of the homogenity of the layer and of only presence of SH-wave. Then, it will be justified that the analysis of waves at our observing point is carried as followings.

It is clear that the function $\tau = \tau_n(\eta)$ implies the arrival time of a wave which is originated from the loaded point $X = L \sin \Omega\eta$ at time η, and which arrives at the observing point after n-time reflections at the interface. Then, the nth term $W_n(0, t)$ in eqn (32) expresses the disturbance due to the reflected wave. (If $n = 0$, it is the direct wave and has no reflections.)

The derivative of the arrival time function is positive for all η and n as the maximum velocity of the load is less than or equal to that of SH-wave of the layer. This is the case (i) and only an ordinary wave of SH-wave propagates in the layer. The wave is originated from the initial position of the load $X = 0$, $Y = -1$, and is reflected at the edges of the layer.

In the case that the maximum velocity is greater than that of SH-wave and that a condition of the case (i) for $n = 0$

$$1/\Omega > \sqrt{L^2+1} - 1 \tag{33}$$

exists, the leading front is generated in the layer but does not pass through the observing point. Hence, the all terms in eqn (32) are given by the form of eqn (21) and the displacement has no singularities.

On the other hand, if we can take a positive integer N given by

$$N = \left[\frac{1}{2}\left\{\frac{\Omega}{2}(L^2 - 1/\Omega^2) - 1\right\}\right], \quad N \geqq 1 \tag{34}$$

where [ ] is the Gauss's symbol and N is the maximum integer that does not exceed the real number in the bracket, the angular frequency Ω satisfies the condition of the case (ii) for $N \geqq n \geqq 0$ and that of the case (i) for $n > N$. Then, the leading front with reflection time up to N passes through the observing point while that having the time greater than N doesn't so. This is easily shown by the comparison of the front $DD'E$ in Fig. 5d with e. The figures show the development with increasing time of wavefronts in the layer loaded as $l\omega/c_1 > 1$. The arrival time of this front is given by $\tau = \tau_n(\eta_j^{(2)})$ and a finite jump takes place in the displacement. That is

$$[W_n(0, t)] = \frac{4(2n+1)}{\{\tau_n(\eta_j^{(2)}) - \eta_j^{(2)}\}^{3/2}\sqrt{2|K_n(\eta_j^{(2)})|}} \times T_n\left(\frac{iL \sin \Omega\eta_j^{(2)}}{\tau_n(\eta_j^{(2)}) - \eta_j^{(2)}}\right); \quad \tau \to \tau_n(\eta_j^{(2)}), \quad j = 1, 2, \ldots \tag{35}$$

where

$$K_n(\eta) = \frac{L^2\Omega^2}{8\sqrt{L^2 \sin^2 \Omega\eta + (2n+1)^2}}\left\{4 \cos(2\Omega\eta) - \frac{L^2 \sin^2(2\Omega\eta)}{L^2 \sin^2 \Omega\eta + (2n+1)^2}\right\} \tag{36}$$

and where $\eta_j^{(2)}$ is given by eqn (25).

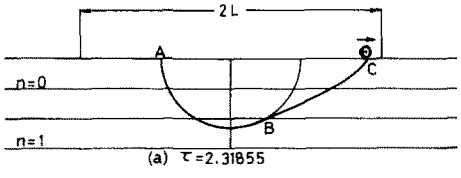

Fig. 5(a).

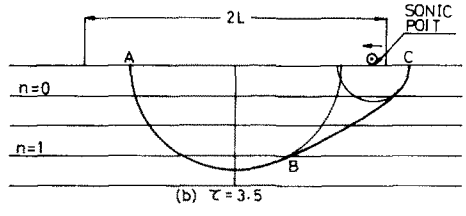

Fig. 5(b).

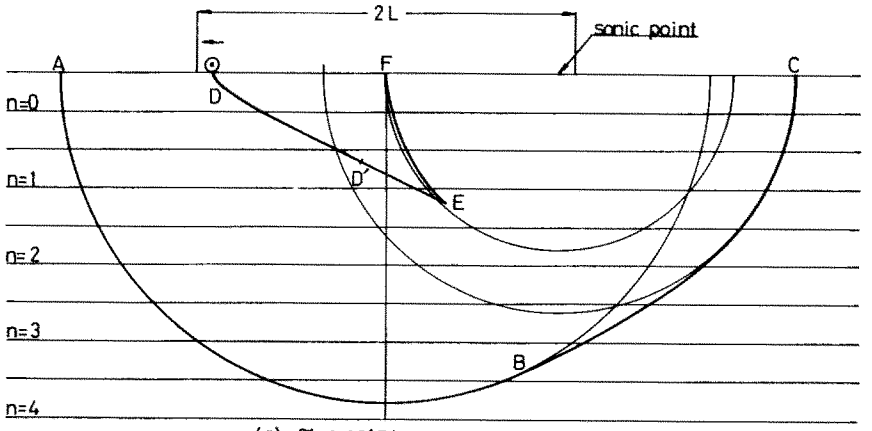

(c) $\tau = 8.60174$

Fig. 5(c).

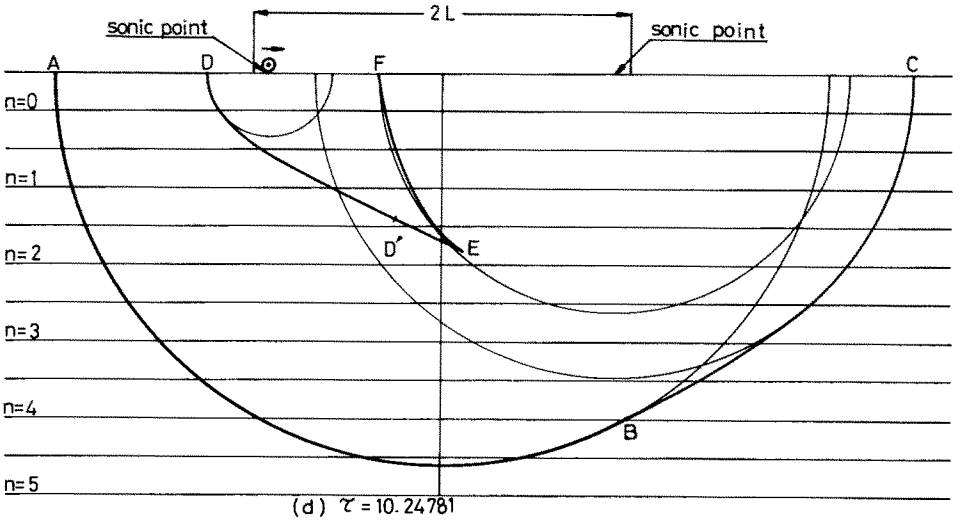

(d) $\tau = 10.24781$

Fig. 5(d).

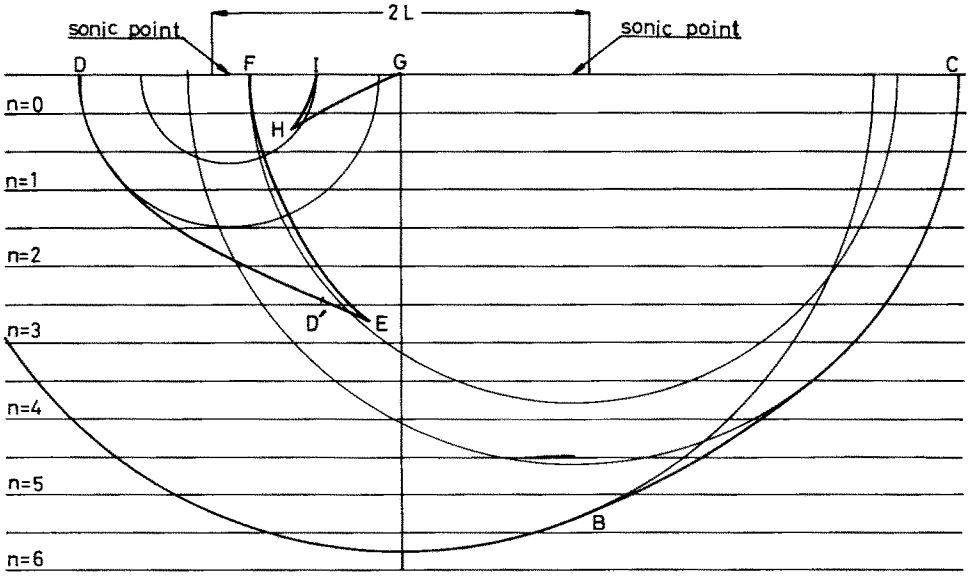

(e) $\tau = 4\pi (=12.56637)$

Fig. 5(e).

Fig. 5. The development with increasing time of wavefronts in the layer that result from a load with $l\omega > c_1$ ($L = 5, \Omega = 0.25$).

On a front emanating from a point, a so-called sonic point, where the velocity of the load comes up to that of SH-wave of the layer, the displacement has not any singularities because the arrival time function $\tau = \tau_n(\eta)$ has no extremum at this point. However, there exists a singular front immediately behind the sonic front. The singular front is generated only when the velocity of the load exceeds that of SH-wave. The behaviour of the arrival of the front at the observing point is recorded in the case (ii), where the arrival time is $\tau_n(\eta_j^{(1)})$ and the singularity is given by

$$W_n(0,t) \simeq \frac{\sqrt{2}(2n+1)}{\{\tau_n(\eta_j^{(1)}) - \eta_j^{(1)}\}^{3/2}} T_n\left(\frac{iL \sin \Omega\eta_j^{(1)}}{\tau_n(\eta_j^{(1)}) - \eta_j^{(1)}}\right)$$

$$\times \log\left\{\eta_j^{(1)} \sqrt{\left|\frac{K_n(\eta_j^{(1)})}{\tau - \tau_n(\eta_j^{(1)})}\right|}\right\}; \quad \tau \to \tau_n(\eta_j^{(1)}) \tag{37}$$

Stronge[10] discussed these characteristics for the problem of the accelerating load, but did not consider the singularities.

As shown in Fig. 5, one of two edges of the singular front coincides with that of the sonic front on the surface of the layer and the other edge is together with that of the leading front in the layer. The condition

$$1/\Omega = \sqrt{(2n+1)^2 + L^2} - (2n+1) \tag{38}$$

states the arrivals of the latter edge, E and H in Fig. 5c–e. The arrival time and the singularity are

$$\tau = \tau_n(\hat{\eta}_j); \quad \hat{\eta}_j = \frac{1}{\Omega}\left\{\pi j + \sin^{-1}\sqrt{\frac{1}{2}(1 - 1/L^2\Omega^2)}\right\}, \tag{39}$$

$$W_n(0,t) \simeq \frac{4\sqrt{3}(2n+1)}{\{\tau_n(\hat{\eta}_j) - \hat{\eta}_j\}^{3/2}\{d^3\tau_n(\eta)/d\eta^3|_{\eta=\hat{\eta}_j}\}^{1/3}}$$

$$\times T_n\left(\frac{iL \sin \Omega\hat{\eta}_j}{\tau_n(\hat{\eta}_j) - \hat{\eta}_j}\right)\{6|\tau - \tau_n(\hat{\eta}_j)|\}^{-1/6}; \quad \tau \to \tau_n(\hat{\eta}_j) \tag{40}$$

where $j = 0$ and 1 stand for the edges, E and H, respectively.

Further, through the above discussions we easily find that there exists no substantial differences between the cases, (ii)–1 and (ii)–2. Only one difference between them is in the point that the arrival time of the singular front given by $\tau_n(\eta_j^{(1)})$ (if $\eta_0 = 2\pi/\Omega$, $j = 1$) is greater in case (ii)–1 and not greater in case (ii)–2 than that of the wave caused from the removal of the load at time η_0.

Now, in order to prove the above fact in graphical forms, numerical calculations are carried out for the displacement. Figure 6 shows the variation with time of the displacement ratio W/W_0. W is the displacement caused by the reciprocating load and is given by eqn (32). W_0 is that caused by a stationary load on the initial position of the reciprocating load and is obtained from eqn (21) with substitution of $\Omega = 0$. It is, of course, non-zero for all time. Results shown in the figure are for $\lambda = 0.25$, $\gamma = 0.5$, $\eta_0 = 4\pi$ and $L = 1, 2, 5$ where $L = 1$ corresponds to the maximum velocity $v_{max} = 0.5c_1$; $L = 2$, $v_{max} = c_1$; $L = 5$, $v_{max} 2.5c_1$. The following conclusions will be summerized from the figure;

(a) The small change at $\tau = 3$ or 5 explains the arrival of the ordinary reflected wavefront and shows that the reflected wave due to the reciprocating load causes less change in the displacement than that due to the stationary load. The change becomes clearer with increase of L because the loaded point at the time $\tau = 3$ or 5 is farther from the observing point with increase of the maximum velocity that is proportional to the amplitude of the reciprocating load. However, this change fades out following the increase of the reflection time rapidly.

(b) The behaviours due to the leading and the singular fronts are shown in the curve $L = 5$ ($v_{max} = 2.5c_1$). As being given by eqns (35) and (37), the leading, singular and their reflected fronts pass through the observing point and the arrivals of them are marked by $J_{n,j}$ and $S_{n,j}$ for the

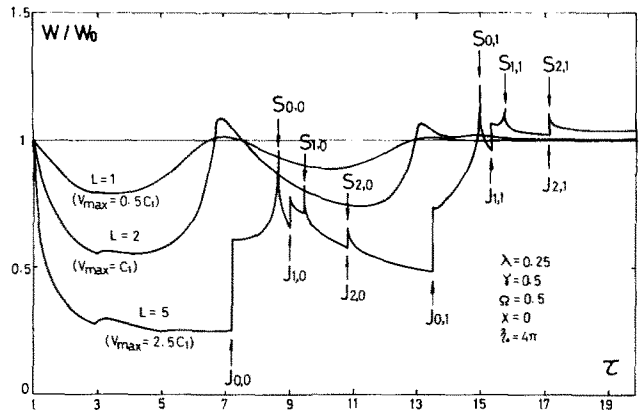

Fig. 6. The variation with time of the displacement ratio W/W_0. $\eta_0 = 4\pi$, $\Omega = 0.5$, $\lambda = 0.25$, $\gamma = 0.5$ (W_0 is for $\Omega = 0$, W is for $\Omega \neq 0$).

leading and singular fronts, respectively. It is easily found that these fronts cause more significant change than the ordinary front in (a), especially, the un-reflected leading fronts $J_{0,0}$ and $J_{0,1}$ would be most. As was expected in Fig. 5, the arrival of the singular front closes to that of the leading front with increase of the reflection time, however, the amplitudes of these are also smaller.

(c) Generally, the curve whose maximum velocity is subsonic varies with time continuously, but, with increasing the velocity the response changes more violently and the delay in phase is more visible.

5. CONCLUDING REMARKS

The technique used in this paper is to employ the transformed boundary condition in the form of integral such as eqn (9) and to reduce the analysis of waves to the examination of the arrival time function $\tau_n(\eta)$. Then, the Cagniard's technique is directly applied to solving the problem of the load with the trigonometric variation of velocity and the result is obtained in terms of single integration.

As the result, in the supersonic case of the maximum velocity the displacement has a finite jump on a leading front and has a logarithmic singularity immediately behind the sonic front. These are given by eqns (35) and (37). The displacement also has the singularity of $0(\Delta\tau^{-1/6})$ as the coincident edge of the leading and singular fronts arrives at the observing point. This is given by eqn (40). Consequently, the wavefront singularity depends on a parameter ν defined by

$$\tau - \tau_n(\eta) \simeq 0(|\eta - \eta^*|^\nu); \quad \eta^* = \tau_n^{-1}(\tau) \tag{41}$$

because the singular part of the integrand in eqn (14) is $\{\tau - \tau_n(\eta)\}^{1/2}$. This implies that the wavefront singularity also depends on the state of the moving load. For the leading and singular fronts $\nu = 2$ and for the coincident edge $\nu = 3$.

Finally, it will be said that our inversion scheme can be used for any problems of the load with arbitrary variation of velocity. For example, if the position of the load is given by a function $\bar{X}(\tau)$ in the dimensionless form, with substitutions of $\bar{X}(\eta)$ into eqns (15) and (16) instead of $L \sin \Omega\eta$ the exact solution can be obtained by following the same way as mentioned in the present paper. The author is now under investigation of the problem of a rotating load on a plane surface of an elastic body as an application of our technique.

Acknowledgements—The author wishes to express his hearty thanks to Prof. A. Atsumi of Tohoku University for his invaluable directions and also to Assist. Prof. T. Ohyoshi of Akita University for his valuable discussions, in the course of the present study. In addition, it should be acknowledged that the expense for the study has been appropriated from the Scientific Research Fund of the Ministry of Education for the fiscal year 1976.

REFERENCES

1. L. Fryba, *Vibration of Solids and Structures under Moving loads*. Nordhoff, Amsterdam (1972).
2. I. N. Sneddon, *Fourier Transforms*. McGraw-Hill, New York (1951).

3. M. Papadopoulus, The use of singular integrals in wave propagation problems; with application to the point source in a semi-infinite media. *Proc. Roy. Soc. London* **A276**, 204 (1963).
4. S. K. Singh and J. T. Kuo, Response of an elastic half space to uniformly moving circular surface load. *J. Appl. Mech.* **37**, 109 (1970).
5. R. G. Payton, An application of the dynamic Betti–Rayleigh reciprocal theorem to moving point loads in elastic media. *Quart. Appl. Math.* **18**, 299 (1960).
6. D. D. Ang, Transient motion of a line load on the surface of an elastic half space. *Quart. Appl. Math.* **18**, 251 (1960).
7. D. C. Gakenheimer and J. Miklowitz, Transient excitation of an elastic half space by a point load traveling on the surface, *J. Appl. Mech.* **36**, 505 (1969).
8. K. I. Beitin, Response of an elastic half space to a decelerating surface point load. *J. Appl. Mech.* **36**, 819 (1969).
9. J. W. Miles, On the response of an elastic half space to a moving blast wave. *J. Appl. Mech.* **27**, 710 (1960).
10. W. J. Stronge, A load accelerating on the surface of an acoustic half space. *J. Appl. Mech.* **37**, 1077 (1970).
11. M. K. Myers, Transient excitation of a liquid half space by a decelerating load. *J. Appl. Mech.* **37**, 475 (1970).
12. T. Ohyoshi, Dynamic stresses produced in an elastic half space by reciprocally moving surface loads. *Trans. Japan Soc. Mech. Engrs.* (in Japanese). To be published.
13. K. Watanabe, Transient response of an elastic half space subjected to a reciprocating anti-plane shear load. *J. Appl. Mech.* (paper No. 76-APM-KK). To be published.
14. J. L. Sackman, A uniform moving load on a layered half plane. *J. Engng. Mech. Div.* **87**, 4 (1961).
15. J. P. Wright and M. L. Baron, Exponentially decaying pressure pulse moving with constant velocity on the surface of a layered elastic material (superseismic layer, subseismic half space). *J. Appl. Mech.* **37**, 141 (1970).
16. L. Knopoff, Love waves from a line SH-source. *J. Geophys. Res.* **63**, 619 (1958).
17. K. Watanabe, Transient contact shear stress in a layered elastic quarter space subjected to anti-plane shear load. *Int. J. Solids Structures* **20**, 75–78 (1977).